CRDV RAPPORT 4202/81
DOSSIER: 3633B-006
AVRIL 1981

DREV REPORT 4202/81
FILE: 3633B-006
APRIL 1981

SURFACE FAILURE OF CO_2 LASER IRRADIATED GLASS

R.W. MacPherson

J.-C. Anctil

Centre de Recherches pour la Défense
Defence Research Establishment
Valcartier, Québec

BUREAU - RECHERCHE ET DEVELOPPEMENT
MINISTERE DE LA DEFENSE NATIONALE
CANADA

NON CLASSIFIÉ
DIFFUSION ILLIMITÉE

RESEARCH AND DEVELOPMENT BRANCH
DEPARTMENT OF NATIONAL DEFENCE
CANADA

CRDV R-4202/81
DOSSIER: 3633B-006

UNCLASSIFIED

DREV R-4202/81
FILE: 3633B-006

SURFACE FAILURE OF CO_2 LASER IRRADIATED GLASS

by

R.W. MacPherson and J.-C. Anctil

CENTRE DE RECHERCHES POUR LA DEFENSE

DEFENCE RESEARCH ESTABLISHMENT

VALCARTIER

Tel: (418) 844-4271

Québec, Canada

April/avril 1981

NON CLASSIFIE

RESUME

L'éventualité de la détérioration du verre chauffé au laser a d'importantes répercussions, tant sur l'étude de la résistance des matériaux soumis aux chocs thermiques que sur la possibilité d'utiliser le laser pour l'usinage et le traitement thermique du verre. Nous décrivons une technique expérimentale permettant d'obtenir la fonction de répartition de la probabilité d'endommagement du verre irradié par un laser et nous développons un modèle qui prédit les distributions de température et de contrainte en fonction du temps. Le modèle théorique ainsi que les résultats expérimentaux montrent que pour des impulsions laser CO_2 inférieures à 1 ms, le processus de détérioration se manifeste sous forme de brisure provoquée par l'effort de tension induit lors du refroidissement subséquent au chauffage d'une mince couche au delà du point de recuit. (NC)

ABSTRACT

The possibility of failure of laser heated glass has important implications in experiments on the thermal shock resistance of materials and in the potential applications of lasers to the machining and heat treating of glass. We describe a method of measuring the damage probability distribution function for laser irradiated glass and develop a model to predict the temperature and stress distributions as a function of time. The experiments and model show that for CO_2 laser pulse lengths inferior to 1 ms, the mode of failure is by fracture under tensile stress induced during cooling after heating a thin layer near the surface beyond the annealing point. (U)

TABLE OF CONTENTS

1.0 INTRODUCTION

Common silica based glasses fail by cracking when irradiated by CO_2 laser pulses at exposure levels above $\sim$ 1 J/cm^2. This phenomenon can be attributed to tensible stresses induced when a thin layer, near the surface, cools down after having been heated above the annealing temperature. A thorough understanding of this effect requires a detailed knowledge of the absorption phenomenon of the CO_2 radiation, the mechanisms of heat transfer, the viscoelastic properties, and the causes of glass failure under stress. These phenomena have important implications in processes involving the assessment of the thermal shock resistance and heat treatment of glassy materials particularly in their laser machining.

To gain an insight into the failure mechanism we conducted a series of experiments designed to measure the irradiation required to initiate damage and we developed a model to predict the observed levels. We adapted the experimental technique of Hacker and Halverson (Ref. 1) for determining the breakdown threshold of glass when irradiated by 100 ns to 100 µs long CO_2 laser pulses. This technique measures the probability distribution function of damage from which we define the threshold as the irradiation required for a 50% probability of damage. With a 1-D thermomechanical model, developed to predict the temperature and stress profiles in irradiated samples, we calculated the irradiation required to cause failure.

This work was performed at DREV between January, 1977, and September, 1980, under PCN 33B06 "Effects of Laser Beams on Materials". This paper was prepared for publication in Proceedings of the Third International Symposium on Gas Flow and Chemical Lasers, les Editions de Physique, Paris, 1980.

2.0 EXPERIMENTAL

Damage was induced by a Laflamme type TEA-CO_2 laser (Ref. 2) modified to produce pulses from 100 ns to 100 μs long, measured at 10% of the maximum pulse power. The available energy ranges from 5 to 50 J depending on the pulse length and the discharge voltage used. The laser operation is multimode on the P20 line with a 50- x 50-mm output beam.

A series of plane and spherical mirrors folded and focussed the beam to produce an approximately 10- x 10-mm spot at the target plane. In addition, a homogenizing reflector, consisting of 32 small flats mounted on a spherical surface, was incorporated to obtain a uniformly distributed beam profile. Beam-splitting wedges of NaCℓ provided sample beams for monitoring the beam energy and profile, the pulse shape, and the spectral content. All angles were kept small to reduce spherical aberration and polarization effects.

We used a multiple-shot, 1-on-1 technique in which each sample site was irradiated once by a pulse from the laser. This avoided cumulative effects which could condition the sample; it thus ensured that the result of each shot was independent of the others. A gas cell attenuator (Ref. 3) varied the laser energy from shot-to-shot, over a narrow range, to obtain about as many damaging shots as undamaging ones.

Damage consisted of a number of fine cracks appearing within 10 s of the laser pulse; it was detected visually by observing a 2 x-magnified image of the site projected onto a ground glass screen with white light. The energy of each shot and the fact that damage occurred or not was recorded in a digital memory. At the end of an experiment,

the data was transferred to DREV main computer for a probit analysis (Ref. 4). This analysis gave maximum likelihood estimates for the mean and standard deviation of the damage probability function. The mean, which corresponds to the irradiation required for a 50% probability of damage, was taken as the threshold. A typical result is shown in Fig. 1 for which the threshold obtained in soda-lime glass was 2.1 J/cm^2 for 11 μs-long pulses.

3.0 MODEL CALCULATIONS

To avoid obscuring the physics of the phenomenon of laser heating and the subsequent induced stress failure in a more complete analysis, we used several simplifying assumptions. Those included the use of uncoupled, quasi-static thermoeleastic theory since the mechanical energy due to stress was much less than the thermal energy and since the relative contribution of dynamic stresses to the total stress was negligible. In calculating the temporal evolution of the temperature distribution in the heated glass we used a 1-D model since the laser radiation was absorbed within a distance much shorter than the dimensions of the laser beam so that variations in the irradiation over the surface were small compared to the variations with depth from the surface. However, the depth of penetration being small compared to the thickness of the material, a solution in a semi-infinite plane was adequate. Furthermore, all thermophysical properties, except viscosity, were assumed to be temperature independent, and heat transfer within the material was assumed to be by diffusion only, i.e. transport by thermal radiation, which significantly occurs only at very high temperatures in glass, was ignored. For the surface boundary condition, we assumed that the rate of heat loss from the surface to the surroundings was proportional to the above ambient temperature. Under these

FIGURE 1 - Experimental results for the measurement of the damage threshold of soda-lime glass irradiated by a 11 μs-long TEA-CO_2 laser pulse at 10.6 μm. The upper left graph is a histogram of all laser shots as a function of laser irradiation (represented by the signal voltage from the energy meter). The lower left graph is a histogram of those shots which damaged the surface. In glass the damage was characterized by the onset of surface cracking. The upper right graph shows the probability for causing damage as a function of laser irradiation. The crosses represent the relative frequencies of damage obtained by dividing the histogram of damaging shots by that of the total number of laser shots. The curve shows the maximum likelihood estimate of the probability where a normal probability density distribution was assumed. The lower right hand graph is a probit plot of the same data. The probit is a coordinate transformation which linearizes the probability curve. The dashed lines represent the 95% confidence limits based on Student's t distribution. The damage threshold corresponding to the 50% probability of damage occurs at 0.242 V which corresponds to an irradiation of 2.1 J/cm^2.

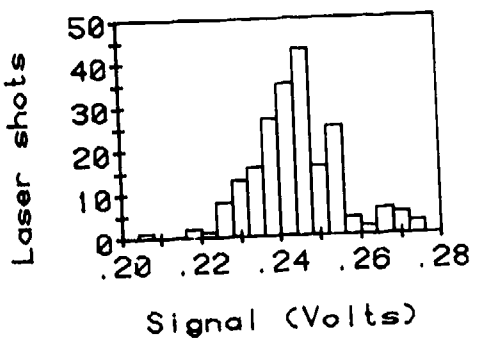
Laser shots
50
40
30
20
10
0
.20 .22 .24 .26 .28
Signal (Volts)

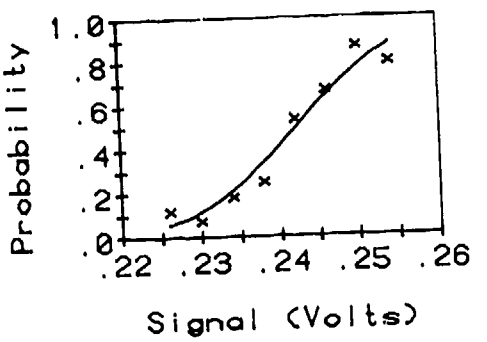
Probability
1.0
.8
.6
.4
.2
.0
.22 .23 .24 .25 .26
Signal (Volts)

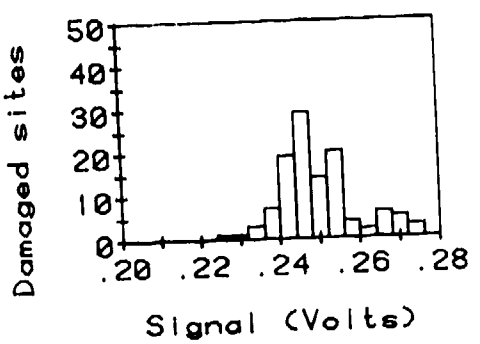
Damaged sites
50
40
30
20
10
0
.20 .22 .24 .26 .28
Signal (Volts)

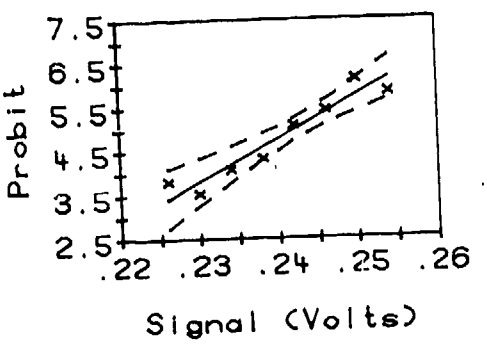
Probit
7.5
6.5
5.5
4.5
3.5
2.5
.22 .23 .24 .25 .26
Signal (Volts)

assumptions, the above ambient temperature, T, satisfies the following equation,

$$\partial^2 T/\partial z^2 - (1/\kappa)\partial T/\partial t + (P_o/k\Lambda)\ \epsilon \exp(-z/\Lambda)\ f(t) = 0 \qquad [1]$$

with the boundary conditions

$$T = T(z,t),\ T(\infty,t) = 0, \qquad [2]$$

$$T(z,0) = 0 \text{ and } k[\partial T(z,t)/\partial z]_{z=0} = h\ T(0,t) \qquad [3]$$

where $\kappa = k/\rho C_p$ is the thermal diffusivity, k is the thermal conductivity, ρ is the density, C_p is the heat capacity, h is a constant describing the surface cooling rate, P_o is the peak laser irradiance *absorbed*, f(t) is the laser pulse waveform normalized so that max f = 1, Λ is the absorption depth of the laser radiation, t is the time, and z is the depth from the surface. The solution resulting from Duhamels' theorem is

$$\psi(z,t) = \int_o^t [\partial \psi_o\ (z,t')/\partial t']_{t'=t-\tau}\ f(\tau)\ d\tau \qquad [4]$$

where $\psi_o(z,t)$ is the solution for a step pulse:

$$\begin{aligned}\psi_o(z,t) = &-\exp.(-a) + F(-a,b) \\ &+[(1+g)/(1-g)]F(a,b) - [2/g(1-g)]F(ag,bg^2) \\ &+[(1+g)/g]\ \text{erfc}\ a/2.\end{aligned} \qquad [5]$$

Here $\psi_o(z,t) = \kappa\rho C_p T(z,t)/P_o\Lambda$, $b = \kappa t/\Lambda^2$, $g = h\Lambda/k$, $a = z/\Lambda$, $F(a,b) = 0.5 \exp(a+b) \operatorname{erfc}(\sqrt{b} + a/2\sqrt{b})$ and erfc (x) is the complementary error function, $(2/\sqrt{\pi})\int_x^\infty \exp(-u^2)\, du$.

In calculating the induced stress (Ref. 5), we assumed that the glass was a standard linear solid with a temperature dependent viscosity, $\eta = \eta_o \exp Q/(T-T_o)$, where η_o, Q, and T_o are constants chosen to fit experimental viscosity data (Ref. 6). Here, T is the actual temperature.

The solution obtained for the stresses is

$$\sigma_{xx} = \sigma_{yy} = \sigma(z,t) = -[E\alpha/(1-\nu)] \cdot \left[T(z,t) - \exp(-P)\int_o^t T(z,\tau)\,\partial P/\partial\tau \exp(P)\, d\tau\right] \qquad [6]$$

where $\partial P/\partial\tau = E/[6(1-\nu)\eta]$, E is Young's modulus, ν is Poisson's ratio and α is the linear expansion coefficient. All the other components of stress, σ_{zz}, σ_{xy}, σ_{xz}, and σ_{yz} equal zero.

4.0 RESULTS AND DISCUSSION

The temperature profile calculated for the experimental pulse of Fig. 2 appears in Fig. 3 where we used C_p = 1254 J/kg.K, Λ = 5 μm, ρ = 2470 kg/m^3, $\kappa = 3.6 \times 10^{-7}$ m^2/s, and h = 3 W/m^2.K (convective losses in still air). We assumed reflection losses of 10%. For times up to $\sim$ 1 ms, the heat is confined to within a depth of $\sim\Lambda$ of the surface.

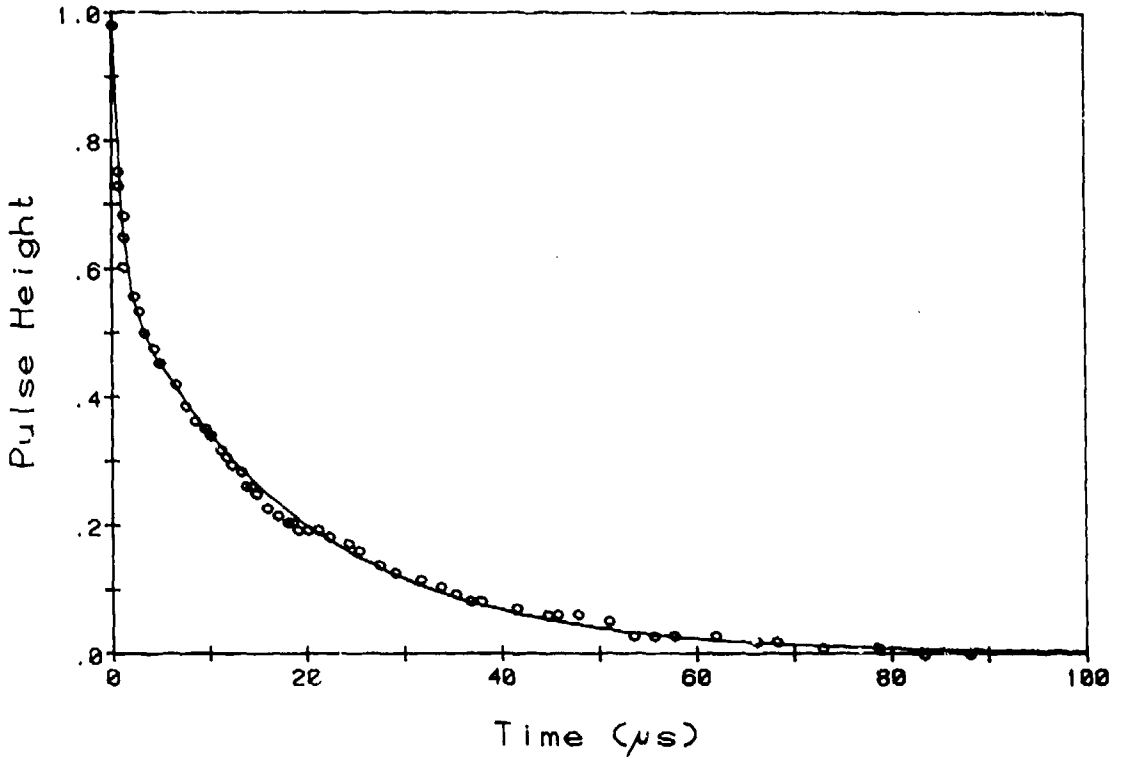

FIGURE 2 - Time evolution of the long pulse. The circles represent points produced by a photon drag detector and measured with an oscillograph. The curve is a least squares fit to a function of the form $f(t) = a_1 \exp(-t/a_2) + a_3 \exp(-t/a_4)$ where $a_1 = 0.591$, $a_2 = 18.4$ μs, $a_3 = 0.409$, and $a_4 = 0.774$ μs. On the time scale of interest here, the rise time of the pulse may be considered instantaneous. The equivalent square pulse length is 11.2 μs.

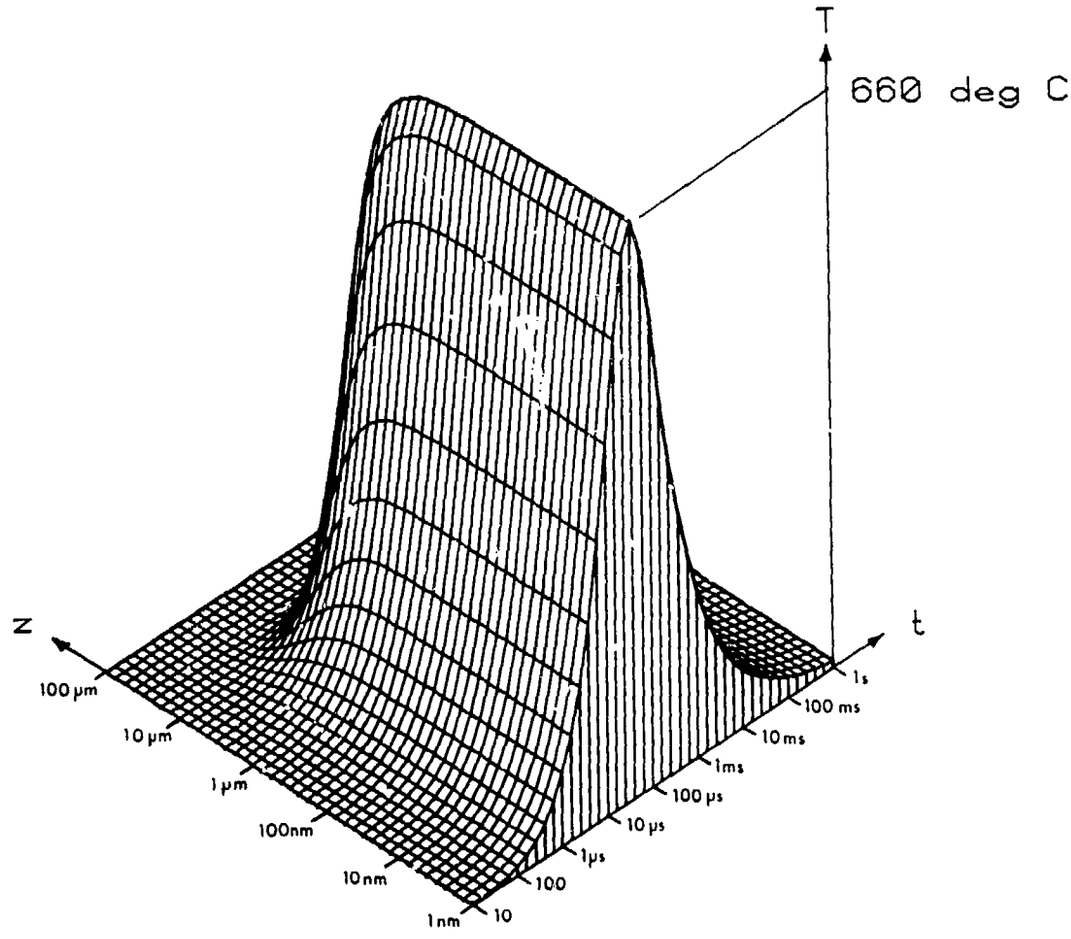

FIGURE 3 - Calculated 1-D temperature profile in soda-lime glass when irradiated by a uniformly distributed CO_2 laser beam at room temperature. The laser irradiation was a 2.1 J/cm^2, 11.2 μs-long pulse with a peak irradiance of 1.95×10^9 W/m^2. The constant values of the thermophysical properties of the glass used are given in the text. The scales of the distance and time axes are expressed in meters and seconds respectively. Note that both axes are logarithmic. The temperature is given in deg C above ambient. The maximum temperature change of 660 deg C was reached at the surface at $\sim$ 40 μs.

As expected in this case, because the rate of surface cooling is low, the maximum temperature occurs at the surface. The temperature then falls relatively slowly during the cooling phase.

The corresponding stress profile appears in Fig. 4. The various thermal and elastic parameters used were: $E = 6.9 \times 10^{10}$ Pa, $\nu = 0.22$, $\alpha = 9.2 \times 10^{-6}$, $\eta_o = 2.38 \times 10^{-6}$ Pa.s, $Q = 18991$ deg C, and $T_o = 48.8°C$. During heating, compressive stress develops throughout the heated volume, its maximum occurring at the surface near the end of the laser pulse. At high temperatures the viscosity of the glass falls sufficiently to allow some of the stress to be relieved by viscous flow. On cooling, the viscosity rapidly increases and thermal contraction produces tensile stress that asymptotically approaches a high value, and is frozen into the glass as it returns to the ambient temperature. This residual stress (Fig. 5) is confined to a thin layer ~ 0.2 Λ deep, near the surface.

We calculated the threshold irradiation required to produce a residual failure stress, σ_{fail}, of 6.9×10^6 Pa. Figure 6 shows the results for square pulses. For pulses shorter than ~ 1 ms, the threshold is approximately constant (within a factor of 2) and thermal diffusion is relatively unimportant.

TABLE I

Failure thresholds for soda-lime glass

Pulse Length τ_p	Threshold irradiation (J/cm^2)	
	Calculated	Measured
492 ns	1.5	1.4
11.2 μs	2.2	2.1

Table I gives the calculated thresholds for the experimental pulse shapes. The pulse lengths refer to equivalent square pulses with the same peak power and total energy ($\tau_p = \int_0^\infty f(t)\, dt/\max f$). These thresholds slightly differ from those calculated for square pulses because the residual stress depends not only upon the temperatures reached but also upon the duration over which the high temperatures are maintained. Since the square pulses deposit all their energy within the pulse time, thermal diffusion effects play a less important role than they do for the real pulse shape and, as a result, we obtain higher temperatures. However, since the real pulses continue to deliver some energy after the pulse time, the high temperatures tend to be maintained for longer times. In the case of square pulses, although the maximum compressive stress is higher and the glass viscosity is momentarily lower, resulting in a higher stress relaxation rate, the overall relaxation achieved may be lower because the time available is shorter than for the real pulses. Which of the two situations produces the larger residual tensile stress depends on the details of each calculation. In general the difference is expected to be small for short pulses. For example, we calculated a 20% larger threshold (2.2 J/cm^2 vs 1.8 J/cm^2 for the equivalent square pulse) for the long experimental pulse whereas the difference was only 2% for the short pulse.

In calculating the damage threshold, the main source of error is in the uncertainty about the absorption depth of CO_2 radiation in glass. Values derived from published optical data (Ref. 7) range from 2 μm to 8 μm. We arbitrarily chose a value of 5 μm, for it lies in the middle of this range. The temperature dependence of the optical, thermophysical, and elastic properties, which was neglected in our calculations, also affects the accuracy of the results. In this respect, the accuracy

FIGURE 4 - Calculated 1-D stress profile in soda-lime glass when heated by the laser pulse described in Fig. 2. The depth from the surface is given in meters and the time axis is in seconds. Note that both axes are logarithmic. By convention, tensile stress is taken as positive and compressive stress negative. Viscoelastic effects were taken into account. The values of the physical properties used are given in the text. On heating, the material undergoes compressive stress due to thermal expansion followed by relaxation in the high temperature regions where the viscosity is low. On cooling, the viscosity increases rapidly and tensile stresses develop because of thermal contraction. In this case, high tensile stresses are confined to a thin, $\sim$ 1-μm, layer next to the surface. At 1 s after the laser pulse, the tensile stress is 3.5×10^5 Pa and it still increases aymptotically to 6.9×10^6 Pa when the temperature returns to ambient. Failure occurs when the tensile stress exceeds the fracture strength of the surface. Since the large stresses develop some time after the laser pulse, failure can occur much later than the time of the laser pulse. Indeed, crack failure was observed to occur in glass up to several seconds after the laser pulse. The high compressive stresses (a maximum of 5×10^8 Pa at 40 μs) produced during the heating phase do not cause failure since the compressive yield stress for glasses is considerably higher than the tensile yield stress.

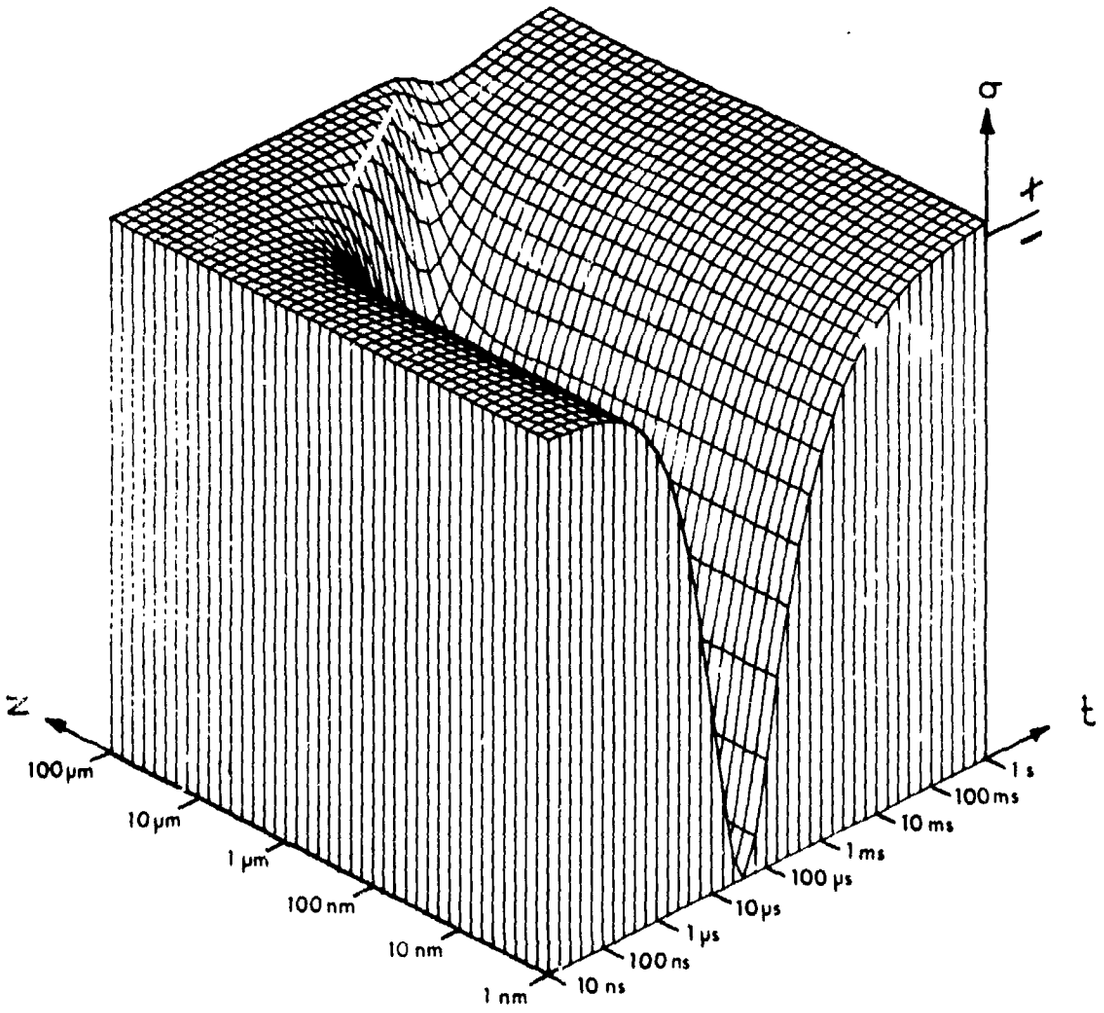
σ
+
−
z
100 μm
10 μm
1 μm
100 nm
10 nm
1 nm
t
10 ns
100 ns
1 μs
10 μs
100 μs
1 ms
10 ms
100 ms
1 s

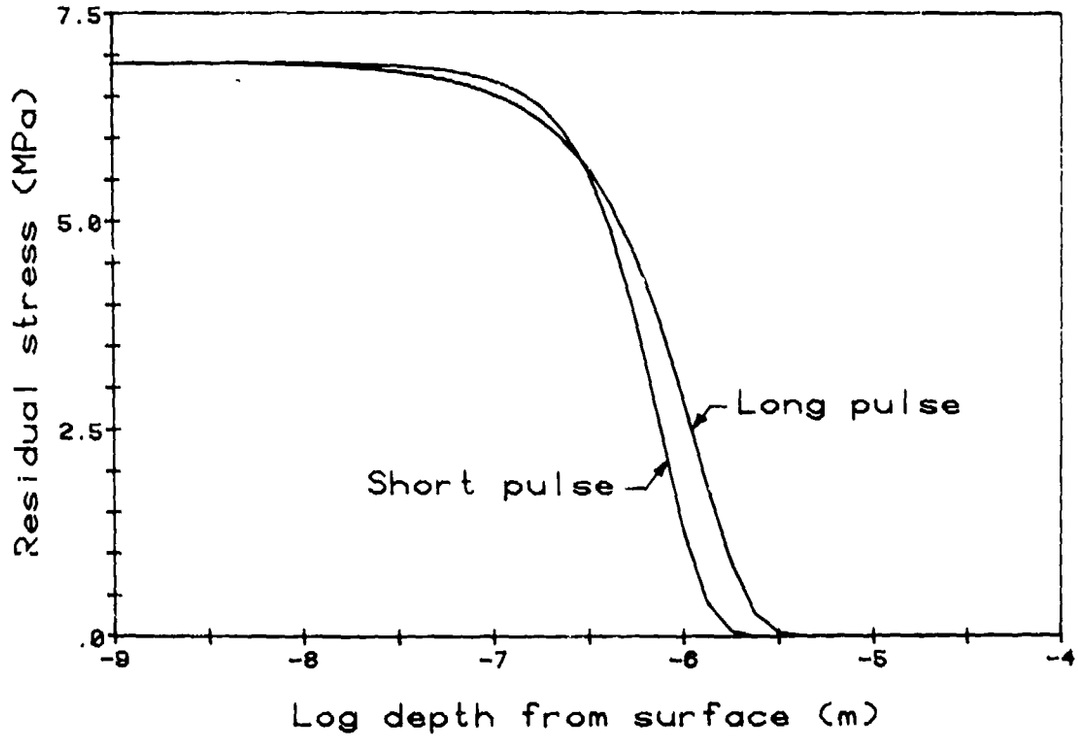

FIGURE 5 - Residual tensile stress as a function of depth from the surface of laser irradiated glass. The curves are from the model predictions calculated for the measured waveforms of the long (11.2 μs) and short (491 ns) pulses. Although the stress produced by the short pulse remains high to a greater depth than that produced by the long pulse, it falls off more abruptly and does not penetrate as deeply. In both cases the stress develops to a depth of ∿ 1 μm or 20% of the 5-μm penetration depth of the CO_2 laser radiation.

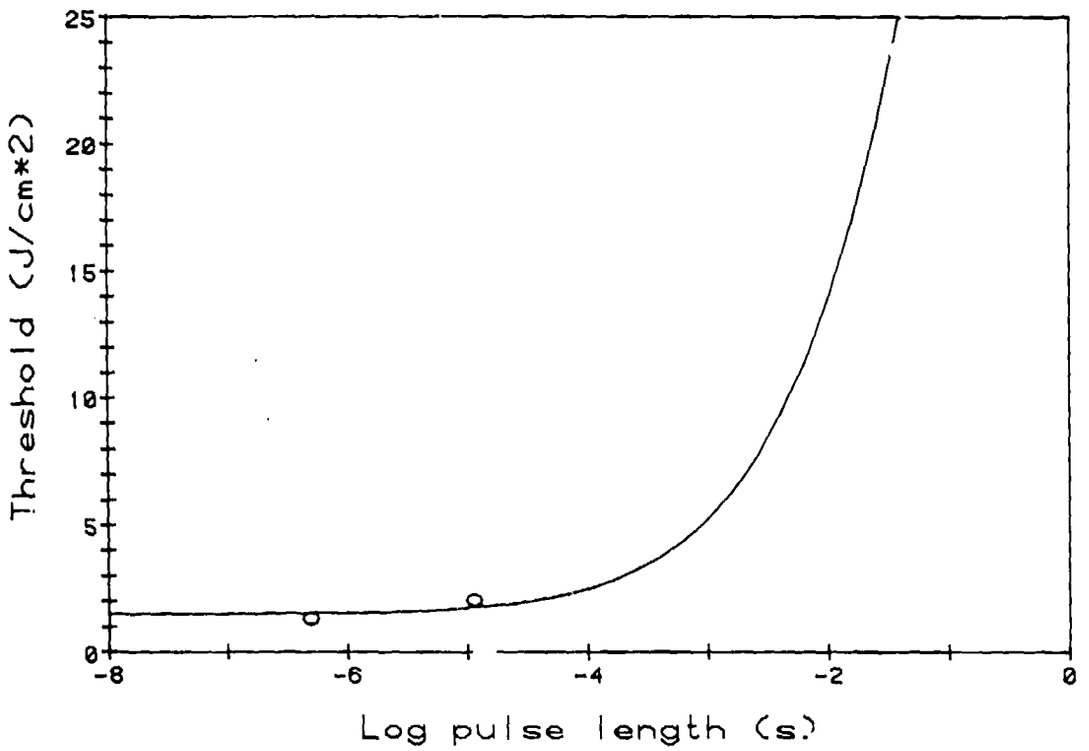

FIGURE 6 - The threshold irradiation calculated from the model for square pulses. The circles represent the measured thresholds for 491 ns and 11.2 μs pulses. Calculations using the actual pulse shape yield estimates of the thresholds closer to the measured values, as shown in Table I.

of our thresholds predictions is somewhat fortuitous. However, the relative thresholds for long and short pulses, and the observation of failure occurring after laser irradiation indicate that the model presents a good explanation of the damage phenomenon.

5.0 CONCLUSION

The residual, tensile stress induced during cooling after irradiation by CO_2 laser pulses, up to 1-ms long, caused glass failure which appeared as surface fracture. At irradiation levels near the threshold, the residual stress is confined to a layer about 20% of the absorption depth. The threshold for damage can be calculated from a 1-D thermomechanical model which accounts for viscoelastic effects and the actual laser pulse shape. The main source of error arises from the uncertainty in the value of the absorption depth.

6.0 ACKNOWLEDGEMENTS

We thank Dr. M. Gravel for many helpful discussions and Mr. C. Trépanier for performing the damage experiments.

7.0 REFERENCES

1. Hacker, M.P. and Halverson, W., "Method for accurate determination of threshold pulse energies for laser-induced gas breakdown", Rev. Sci. Instrum., Vol. 47, p. 634, 1976.

2. Laflamme, A.K., "Double discharge excitation for atmospheric pressure CO_2 lasers", Rev. Sci. Instrum., Vol. 41, pp. 1578-1581, 1970.

3. MacPherson, R.W., "Variable attenuator for TEA-CO_2 lasers", Rev. Sci. Instrum., Vol. 45, pp. 316-317, 1974.

4. Finney, D.J., "Probit analysis", Cambridge University Press, Cambridge, 1952.

5. Boley, B.A. and Weiner, J.H., "Theory of thermal stresses", New York, John Wiley and Sons, Inc., 1960.

6. Corning Glass Works, Advanced Products Department, Technical Products Division, "Material Handbook", Eighth Edition, December 1978.

7. Delisle, C. and Girard, A., "Etude de la pénétration des rayonnements infrarouges dans des substances diélectriques opaques", Université Laval, Laboratoire de recherches en optique et laser, 1979.

DREV R-4202/81 (UNCLASSIFIED)

Research and Development Branch, DND, Canada.
DREV, P.O. Box 8800, Courcelette, Que. G0A 1R0

"Surface Failure of CO_2 Laser Irradiated Glass"
by R.W. MacPherson and J.-C. Anctil

The possibility of failure of laser heated glass has important implications in experiments on the thermal shock resistance of materials and in the potential applications of lasers to the machining and heat treating of glass. We describe a method of measuring the damage probability distribution function for laser irradiated glass and develop a model to predict the temperature and stress distributions as a function of time. The experiments and model show that for CO_2 laser pulse lengths inferior to 1 ms, the mode of failure is by fracture under tensile stress induced during cooling after heating a thin layer near the surface beyond the annealing point.

DREV R-4202/81 (UNCLASSIFIED)

Research and Development Branch, DND, Canada.
DREV, P.O. Box 8800, Courcelette, Que. G0A 1R0

"Surface Failure of CO_2 Laser Irradiated Glass"
by R.W. MacPherson and J.-C. Anctil

The possibility of failure of laser heated glass has important implications in experiments on the thermal shock resistance of materials and in the potential applications of lasers to the machining and heat treating of glass. We describe a method of measuring the damage probability distribution function for laser irradiated glass and develop a model to predict the temperature and stress distributions as a function of time. The experiments and model show that for CO_2 laser pulse lengths inferior to 1 ms, the mode of failure is by fracture under tensile stress induced during cooling after heating a thin layer near the surface beyond the annealing point.

DREV R-4202/81 (UNCLASSIFIED)

Research and Development Branch, DND, Canada.
DREV, P.O. Box 8800, Courcelette, Que. G0A 1R0

"Surface Failure of CO_2 Laser Irradiated Glass"
by R.W. MacPherson and J.-C. Anctil

The possibility of failure of laser heated glass has important implications in experiments on the thermal shock resistance of materials and in the potential applications of lasers to the machining and heat treating of glass. We describe a method of measuring the damage probability distribution function for laser irradiated glass and develop a model to predict the temperature and stress distributions as a function of time. The experiments and model show that for CO_2 laser pulse lengths inferior to 1 ms, the mode of failure is by fracture under tensile stress induced during cooling after heating a thin layer near the surface beyond the annealing point.

DREV R-4202/81 (UNCLASSIFIED)

Research and Development Branch, DND, Canada.
DREV, P.O. Box 8800, Courcelette, Que. G0A 1R0

"Surface Failure of CO_2 Laser Irradiated Glass"
by R.W. MacPherson and J.-C. Anctil

The possibility of failure of laser heated glass has important implications in experiments on the thermal shock resistance of materials and in the potential applications of lasers to the machining and heat treating of glass. We describe a method of measuring the damage probability distribution function for laser irradiated glass and develop a model to predict the temperature and stress distributions as a function of time. The experiments and model show that for CO_2 laser pulse lengths inferior to 1 ms, the mode of failure is by fracture under tensile stress induced during cooling after heating a thin layer near the surface beyond the annealing point.